Research Square

Preprints are preliminary reports that have not undergone peer review.
They should not be considered conclusive, used to inform clinical practice,
or referenced by the media as validated information.

Temperature and Strain Rate Effects on the Strength of Carbyne-Graphene Nanoelements: An Atomistic Fluctuation Model and MD-simulation

Sergiy Kotrechko
G.V. Kurdyumov Institute for Metal Physics
Oleksandr Ovsiannikov
G.V. Kurdyumov Institute for Metal Physics
Mykhailo Barvinko
misagig@gmail.com
G.V. Kurdyumov Institute for Metal Physics

Research Article

Keywords: Carbyne, Graphene, Nanoelements, Strength, Strain rate, Temperature effect, Molecular dynamics, Straintronics

Posted Date: May 27th, 2026

DOI: https://doi.org/10.21203/rs.3.rs-9616193/v1

License: This work is licensed under a Creative Commons Attribution 4.0 International License.
Read Full License

Additional Declarations: No competing interests reported.

Temperature and Strain Rate Effects on the Strength of Carbyne-Graphene Nanoelements: An Atomistic Fluctuation Model and MD-simulation

S. Kotrechko[1], O. Ovsiannikov[1], Corresponding author: M. Barvinko[1]
[1]G.V. Kurdyumov Institute for Metal Physics, Kyiv, Ukraine

Corresponding author email: misagig@gmail.com

Abstract

A theoretical framework describing the atomistic influence of temperature and strain rate on the strength of nanoelements composed of combinations of one- and two-dimensional structures are developed. In particular, carbyne–graphene nanoelements (CGNs), consisting of graphene sheets connected by a carbyne chain lying in the plane of these sheets, are considered.

A fluctuation-based strength model is proposed, demonstrating that temperature and strain rate effects are governed by fluctuation-induced rupture of contact bonds. The dependencies of CGN strength on temperature and strain rate are obtained and verified by molecular dynamics simulations using the machine-learning based atomic cluster expansion (ML-ACE) potential.

It is shown that the temperature sensitivity of CGN strength is comparable to that of graphene but significantly lower than that of metallic nanowires, due to the high stiffness of sp-bonds. The relatively weak dependence of strength on temperature and strain rate highlights the potential of CGNs for applications in straintronic devices.

Keywords

Carbyne; Graphene; Nanoelements; Strength; Strain rate; Temperature effect; Molecular dynamics; Straintronics;

Introduction

Monatomic carbon chains are considered ideal one-dimensional conductors and the thinnest possible interconnects for prospective nanodevices [1–3]. Therefore, carbynes can be used in future devices such as transport channels, on-chip interconnects for molecular electronics, and spintronic nanodevices [4–6].

Typically, the mechanical properties of carbyne and graphene are studied for isolated objects: carbyne as an infinite chain [7], a ring [8-10], or a finite chain terminated with single hydrogen or metal atoms at the ends [10-11]. Such studies make it possible to obtain the properties of ideal polyyne and cumulene, although in real objects atomic chains are terminated by other carbon structures, usually two-dimensional ones [5, 12]. The possibility of practical application of the unique physical and mechanical properties of carbyne chains is associated with carbyne–graphene nanoelements (CGNs), which consist of two graphene sheets connected by a chain lying in the plane of these sheets. At present, such a structure is considered a promising element of straintronics [13-15], since its deformation leads to a change in the band gap width and, accordingly, its functional properties. In particular, this is promising for use in optoelectronic devices with tunable wavelengths [16].

Experimental studies of the conductivity of CGNs and the metal–semiconductor transition under tensile deformation have been carried out [5,16,17]. In [18], it was demonstrated that the combination of electrical and magnetic properties of the chains and contacts leads to the creation of nanodevices with exceptional spintronic properties, such as the coexistence of magnetic and semiconducting behavior. Interesting tunable properties of carbon chains integrated with sp^2 carbon are discussed in detail in [19].

The efficiency of practical application of straintronic elements largely depends on the range of allowable operating deformations and temperatures, the prediction of which requires physical insight into the atomic mechanisms of their deformation and failure. A key feature of these mechanisms is the fluctuation-induced rupture of contact bonds. The Arrhenius reaction rate theory, in its various modifications, is commonly used to analyze thermally activated processes [20-23]. The main limitation of its application is the need to determine coefficient values based on experimental data. For nano-objects, this implies significant experimental challenges. Therefore, one direction for improving statistical models is the elimination of fitting constants. In particular, attempts have been made to use results of density functional theory (DFT) calculations to obtain information about atomic interactions in nanoelements [16].

A characteristic feature of these and other statistical models is that they allow prediction of the lifetime of mechanically unloaded nanosystems. However, force fields generated by deformation are an essential attribute of straintronic elements. The main idea of the existing approach to accounting for the influence of force fields on bond rupture waiting time is that the energy barrier height decreases under the action of force. A linear law of barrier reduction is usually assumed. The coefficient before the stress term is treated as a material constant – the activation volume. This approach was originally proposed for predicting the durability of macroscopic 3D systems [24].

At present, attempts are being made to apply this approach to nano-objects as well [25]. However, nanoscale systems exhibit a characteristically nonlinear dependence of the energy barrier height on the applied stress level [25,26].

In [27], a fluctuation-based approach was proposed for predicting the probability of contact bond rupture in CGNs and similar one- and two-dimensional nanostructures. According to this approach, reaching a critical magnitude of fluctuation is a necessary condition for bond rupture. This critical value is determined by the level of force acting within the nanoelement. Within this framework, a fluctuation model was developed that makes it possible to predict the temperature dependence of both the mean value and the scatter range of CGN lifetime over a wide range of loads [28,29].

In the present work, a further step is taken: a fluctuation-based *strength* model is proposed for nanoelements subjected to a constant strain rate. Atomic-scale mechanisms are identified, and the regularities of the influence of temperature and strain rate on the strength of carbyne-graphene nanoelements are established. The proposed model is validated based on molecular dynamics simulations over a wide range of temperatures and strain rates. The ranges of temperatures and strain rates that enable the application of CGNs in nanoelectronic and straintronic devices are determined.

Existing approaches to predicting the strength and lifetime of nanostructures attempt to transfer macroscopic fracture models (the Zhurkov model and the Bailey principle) to the nanoscale. However, such an approach is not suitable for one- and two-dimensional nanostructures, since the Zhurkov model does not account for the nonlinearity of tensile deformation, while the Bailey approach essentially describes fracture as a result of damage accumulation. In contrast, in the case of CGNs, the critical event is the rupture of a single *contact* bond.

MD-simulation

Molecular dynamics (MD) is a powerful tool for studying nanoscale systems, enabling direct analysis of atomic structure evolution over a wide range of temperatures and strain rates.

However, a significant challenge remains the accurate parameterization of interatomic potentials for configurations containing different allotropes of carbon. As a result, attempts to numerically model graphene-carbyne contacts have often led to results that contradict first-principles DFT calculations [30].

In recent years, significant progress has been achieved in the development of interatomic potentials and methods for their construction, which enable the description of covalent bonds with accuracy comparable to DFT, thereby opening the possibility for adequate MD simulation of combined one- and two-dimensional carbon nanostructures [31,32].

Simulations were performed for a carbyne-graphene nanoelement (CGN) consisting of two graphene sheets measuring 15.6 Å × 32.0 Å, connected by a carbyne chain. The graphene sheets lie in the same plane with a zigzag orientation along the direction of tensile loading of the nanoelement, while the carbyne chain is parallel to the corresponding direction in graphene (Fig. 1). The number of atoms in the carbyne chains varied from 6 to 18, in increments of four atoms.

Molecular dynamics (MD) simulations were performed using the LAMMPS software package [33]. The ML-ACE type interatomic potential was chosen for the calculations [31,34]. The ACE potential was parameterized based on a dataset of relevant carbon structures over an extended range of volumes and energies, obtained using density functional theory (DFT). This potential was selected due to its high accuracy in reproducing the structural and mechanical properties of both crystalline and amorphous carbon phases [32]. It is also consistent with the results of DFT calculations [35].

The integration of the equations of motion was carried out with a time step of 10^{-15} s. Temperature control was implemented using the Nosé–Hoover thermostat [37] with a damping parameter T_{damp} = 0.20, corresponding to a relaxation time constant of 200 simulation steps(2×10^{-13}s).

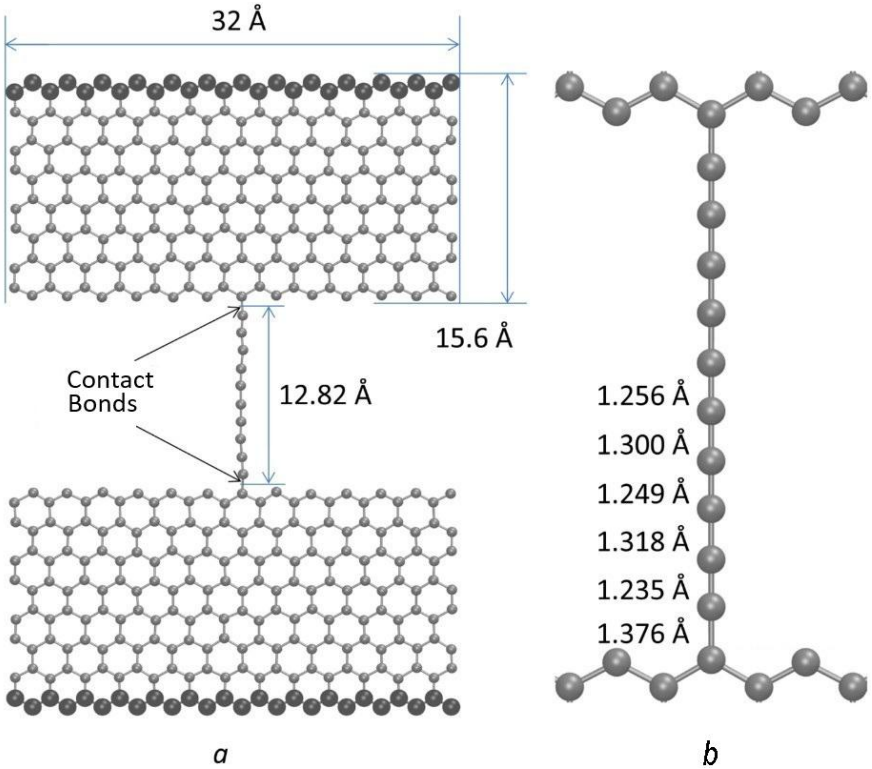


Fig. 1. (a) CGN sample; atoms acting as grips are indicated by larger spheres. (b) Interatomic distances in a carbyne chain consisting of 10 atoms;

Tensile loading was applied at a constant strain rate by elongating the simulation cell. At the edges of the simulation cell, atoms were kept fixed, thus acting as “grips.” This approach ensures a quasi-static deformation regime, in which the system has sufficient time to relax after each increment of strain.

The values of coordinates, velocities, and virial stresses were recorded every 10-time steps. The stress applied to the chain was calculated from the sum of the virial stresses of the atoms [37].

$$\sigma_{ch}^{\alpha\beta} = \frac{1}{2V_{ch}} \sum_{i}^{i \in ch} \xi_i^{\alpha\beta} \quad (1)$$

Where $\alpha, \beta = \overline{x, y, z}$ are the indices of the stress tensor components; $\sigma_{ch}^{\alpha\beta}$ - the stress in the chain; $\xi_{ch}^{\alpha\beta}$ - the virial stress on the *i*-th atom; the summation is performed over the atoms within the chain.

$$\xi_i^{\alpha\beta} = -2m_i v_\alpha \cdot v_\beta + \sum_{i \neq j}^{N} r_{ij}^{\alpha} \cdot f_{ij}^{\beta} + \frac{1}{3} \sum_{j,k \neq i}^{N} \left(r_{ij}^{\alpha} \cdot f_{ijk}^{\beta} + r_{ij}^{\alpha} \cdot f_{ijk}^{\beta} \right) + \frac{1}{4} \sum_{j,k,l}^{N} \left(r_{ij}^{\alpha} \cdot f_{ijkl}^{\beta} + r_{ik}^{\alpha} \cdot f_{ijkl}^{\beta} + r_{ik}^{\alpha} \cdot f_{ijkl}^{\beta} \right) \quad (2)$$

where r_{ij}^{α} is the distance between atoms *i* and *j*; f_{ij}^{β} - is the force of the pairwise interaction between atoms *i* and *j*;f_{ijk}^{β}- is the force of the three-body interaction among atoms *i*, *j,* and *k*;f_{ijkl}^{β} is the force of the four-body interaction among atoms *i*, *j,* and *l.*

For a one-dimensional object such as the carbyne chain, strength is most appropriately expressed in units of force. Accordingly, from Eq. (1) we obtain:

$$F = \frac{1}{2L_{ch}} \sum_{i}^{i \in ch} \xi_i^{yy} \quad (3)$$

At finite temperatures, the force F given by Eq.3 includes contributions from all local fluctuations, introducing significant noise into both the instantaneous force and its critical value (Fig. 2).

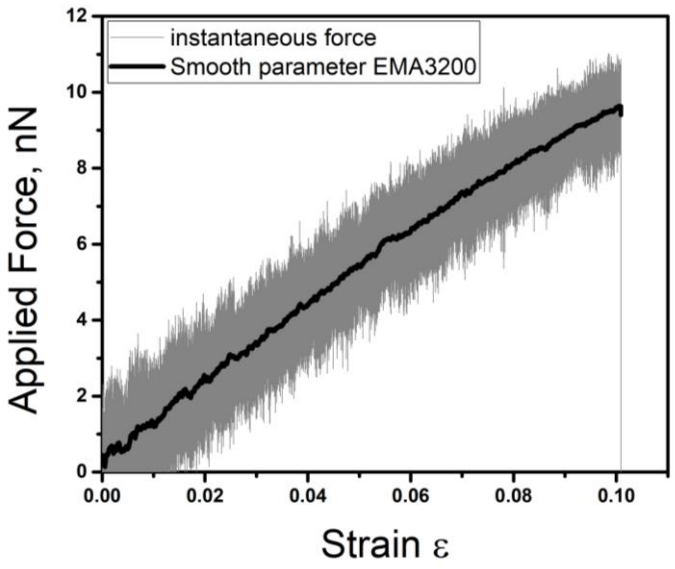


Fig. 2 Dependence of the applied force on the strain of the CGN with a 10-atom chain at a temperature of 600 K and a loading rate of 0.01 m/s

To mitigate this effect, the exponential moving average (EMA) method was used. The choice of the EMA parameter represents a trade-off: a higher value produces a smoother curve and more effectively suppresses noise, but at the same time leads to a greater underestimation of the mean value relative to the effective value at a given point.

For a tensile rate of 1 m/s, an EMA parameter value of 200 was used, and it was increased proportionally with decreasing rate; for example, for 0.1 m/s, EMA = 2000. With further reduction in the rate, the limiting value was 3200; further increase does not provide any additional effect (Table 1).

Chains with an even number of atoms were chosen to ensure consistent alternation of long and short bonds along the entire chain (Fig. 1b), given that the contact bonds are expected to be “long.” This can be interpreted as longer distances corresponding to single covalent bonds, while shorter ones correspond to triple bonds.

For chains containing 6, 14, and 18 atoms, the tensile rate was scaled so as to preserve the strain rate of the chain (Table 1).

Table 1. Tensile loading parameters for carbyne chains of different lengths.

Number of atoms	Initial chain length	Tensile velocity *v*, м/с	Strain rate $\dot{\varepsilon}$, c^{-1}.	**EMA smoothing parameter**
6	7.73	0.006	$7.8 \cdot 10^6$	3200
		0.060	$7.8 \cdot 10^7$	2000
		0.600	$7.8 \cdot 10^8$	200
10	12.82	0.01	$7.8 \cdot 10^6$	3200
		0.10	$7.8 \cdot 10^7$	2000
		1.00	$7.8 \cdot 10^8$	200
14	17.95	0.014	$7.8 \cdot 10^6$	3200
		0.140	$7.8 \cdot 10^7$	2000
		1.400	$7.8 \cdot 10^8$	200
18	23.06	0.018	$7.8 \cdot 10^6$	3200
		0.180	$7.8 \cdot 10^7$	2000
		1.800	$7.8 \cdot 10^8$	200

Comparison of the simulation results for a system with a large graphene region (Fig. 1) and a smaller one (Fig. 3) justified the possibility of using samples with a reduced total number of atoms. Thus, the model system contained 48 atoms instead of 426, which made it possible to significantly accelerate the calculations and increase statistical sampling.

To obtain more accurate average values for each temperature, more than 50 simulations were performed with different initial distributions of atomic velocities.

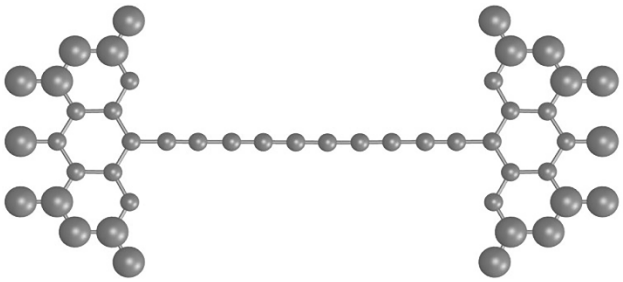


Fig.3. A sample with a reduced contact region; the grip atoms are indicated by large spheres.

Fluctuation model

According to [27], the rupture strength of a contact bond in the chain is determined by the critical fluctuation δ_c of its length at which rupture occurs under a given applied force F_f

(Fig. 4). Thus, the value of the critical fluctuation δ_c is determined by the magnitude of the applied force F_f.

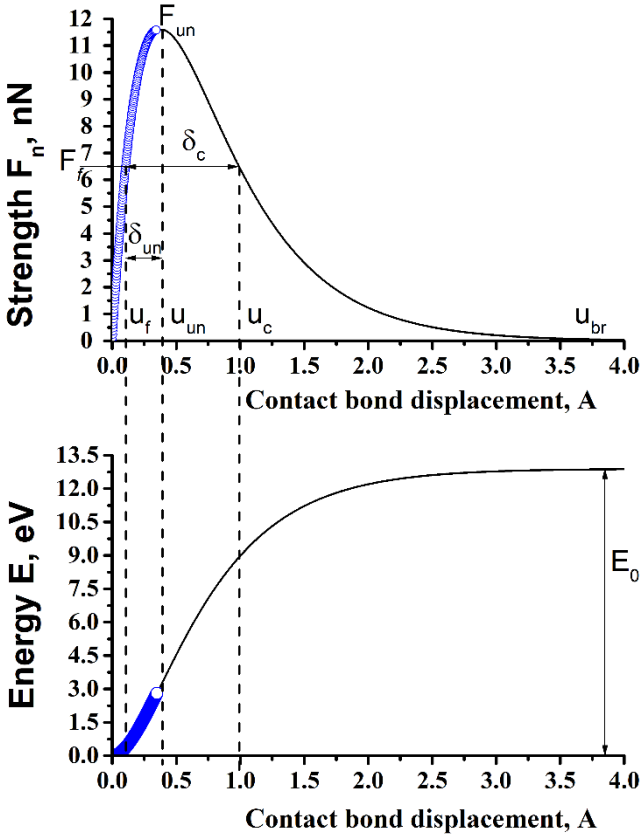


Fig. 4. Deformation diagram of the contact bond (Fig. 1a) and the dependence of the interatomic interaction energy *E* on the contact bond length (schematic): F_f – applied force; u_f – displacement of an atom from its equilibrium position under mechanical loading; F_{un} and u_{un} – force and displacement corresponding to the instability of the contact bond, respectively; δ_{un} – fluctuation associated with bond instability; u_c and δ_c – critical displacement and critical fluctuation, respectively; u_{br} – displacement at which bond rupture occurs; E_0– depth of the potential well.

If the applied force F_f reaches the limiting value F_{un}, a non-fluctuational (athermal) mechanism of interatomic bond rupture takes place. At lower levels of loading, fracture initiation is possible only due to thermal fluctuations. However, for such fluctuations to result not merely in temporary instability of the interatomic interaction but in complete bond rupture, the atomic displacement must reach or exceed a critical value u_c.
This value is determined both by the magnitude of the applied load $F_f$and by the nature of the decrease in interatomic force within the displacement range $u_{un} \leq u \leq u_{br}$. As the applied load F_f decreases, the required magnitude of the critical fluctuation δ_c increases (Fig. 4).
According to the proposed approach for predicting the probability of rupture of a CGN contact bond within one oscillation period [39]:

$$P(\delta \geq \delta_c) = \frac{1}{Z}\int_{\delta_c}^{\delta_{br}} exp\left[-\frac{E(u_f+\delta)-E(u_f)}{k_B T}\right] d\delta \quad (4)$$

Where Z – statistical sum

$$Z = \int_{0}^{\delta_{br}} exp\left[-\frac{E(u_f+\delta)-E(u_f)}{k_B T}\right] d\delta \quad (5)$$

k_B is the Boltzmann constant, δ_{br} the fluctuation required for rupture of the contact bond in the absence of an applied force, and T – the temperature.

As shown in [29], the integral in Eq. (4) cannot be expressed in terms of elementary functions; however, an approximate expression for Eq. (4) can be written as follows:

$$P(\delta \geq \delta_c) \approx exp\left[-\frac{E(u_f+\delta)-E(u_f)}{k_B T}\right] \quad (6)$$

Accordingly, at zero applied force, Eq. (6) reduces to the classical Arrhenius relation:

$$P(\delta \geq \delta_c) \approx exp\left[-\frac{E_0}{k_B T}\right] \quad (7)$$

According to [39], the interatomic interaction energy in the *contact* bond and its deformation diagram can be approximated with sufficient accuracy by a Morse-type relation.

$$E(u) = E_0(e^{-2bu} - 2e^{-bu}) \quad (8)$$

Accordingly, the expression for the deformation diagram of the contact bond can be expressed as follows:

$$F(u) = 2bE_0(e^{-bu} - e^{-2bu}) \quad (9)$$

Where E_0 – the depth of the potential well, b – the function parameter, u – the elongation of the contact bond.

This enables an analytical expression to be obtained for the probability of fracture of the contact bond under a given applied force during a single atomic vibration period. Taking Eqs. (8)-(9) into account, Eq. (6) can be written as:

$$P(\delta \geq \delta_c) = P_0(F) = exp\left[-\frac{E_0}{k_B T}\left(\sqrt{1-\frac{F(u)}{F_{un}}} - \frac{F(u)}{2F_{un}} ln\left[\frac{1+\sqrt{1-\frac{F(u)}{F_{un}}}}{1-\sqrt{1-\frac{F(u)}{F_{un}}}}\right]\right)\right] \quad (10)$$

Where F – the applied force

When the CGN is stretched at a constant strain rate, the force acting on the contact bond increases from zero until rupture occurs. Accordingly, the probability of fracture of the CGN at the n-th loading step is defined as the probability of rupture of the contact bond at that step, provided that rupture has not occurred during any of the preceding loading steps:

$$P_n = P_0(F_n) \prod_{i=1}^{n-1}(1 - P_0(F_i)) \quad (11)$$

For computational purposes, this relation can conveniently be represented in the following form:

$$P_n = P_0(F_n)\, exp[\sum_{i=1}^{n-1} ln(1 - P_0(F_i))] \quad (12)$$

In this expression, the force at the n-th loading step is determined from Eq. (9), taking into account the increment in the contact bond length during one atomic vibration period:

$$u_n = \mathrm{n}\mathrm{V}\tau_0 \quad (13)$$

Where n – number of an atomic vibration, V – tensile velocity, τ_0 – atomic vibration period.

Results and the discussion

A distinctive feature of the proposed model is the absence of fitting constants. Information about the properties of the contact bond is specified by its deformation curve (Fig. 4), which is obtained from molecular dynamics (MD) simulations of tensile loading of the CGN at T=3K. Such a low temperature makes it possible to model its quasi-static tension with sufficient accuracy without taking thermal fluctuations into account. Approximating this curve by relation (9) makes it possible to determine the values of the parameters E_0 and *b*. In the present case, for the contact bond $E_0 = 13.18 \cdot 10^{-19} J; b = 1.78 \dot{A}^{-1}$.

The theoretical temperature relations are in good agreement with the results of molecular dynamics (MD) simulations (Fig. 5). The slight deviation of the theoretical values of F_c, from the MD simulation results is due to the fact that, for the sake of simplicity, the model assumes that the applied force acting on the contact bond remains constant during the fluctuation event. In reality, when a fluctuation occurs, some relaxation of the applied force may take place if the energy accumulated in the stretched chain is insufficient to maintain a constant value of the acting force.

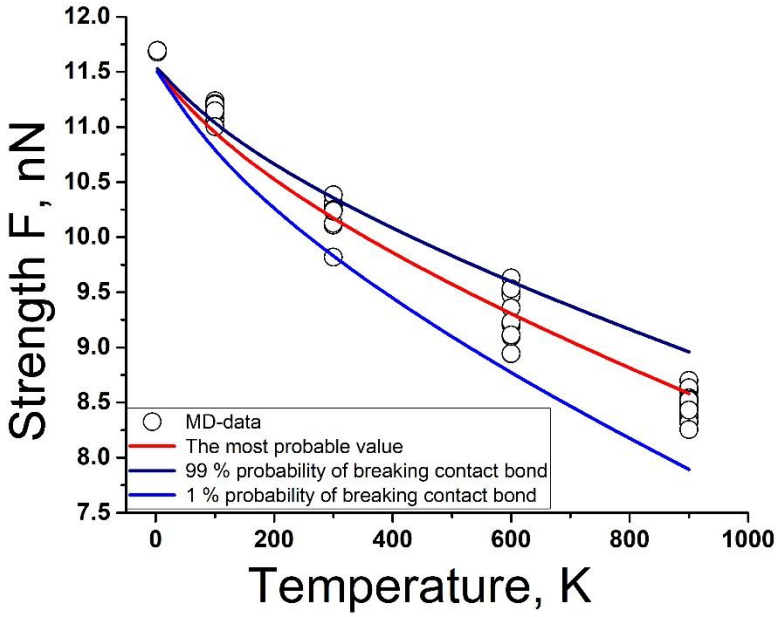


Fig. 5. Temperature dependence of the strength of a carbyne–graphene nanoelement containing an 18-atom chain at a tensile loading rate of 0.01 m/s: circles – MD simulation results; lines – theoretical predictions.

Effect of temperature

With increasing temperature, the CGN strength decreases approximately linearly (Fig. 6), in agreement with the available data, particularly those reported in Ref. [30]. According to the proposed model, the temperature dependence of the contact bond strength is explained by the increase in the probability of occurrence of the critical fluctuation δ_c required for bond rupture under an applied force lower than the bond strength F_{un} (Fig. 4).

The maximum reduction in strength at temperatures up to 900 K and at the minimum stretching rate of 0.01 m/s does not exceed 20%. In terms of order of magnitude, this is close to the values reported for graphene (27%) [31], but significantly smaller than that for metallic nanowires (50%) [32]. This can primarily be attributed to the high stiffness of the interatomic bonds in the carbyne chain.

The temperature dependences of the strength of the CGN for different strain rates and different numbers of atoms in the carbyne chain are presented in Fig. 6.

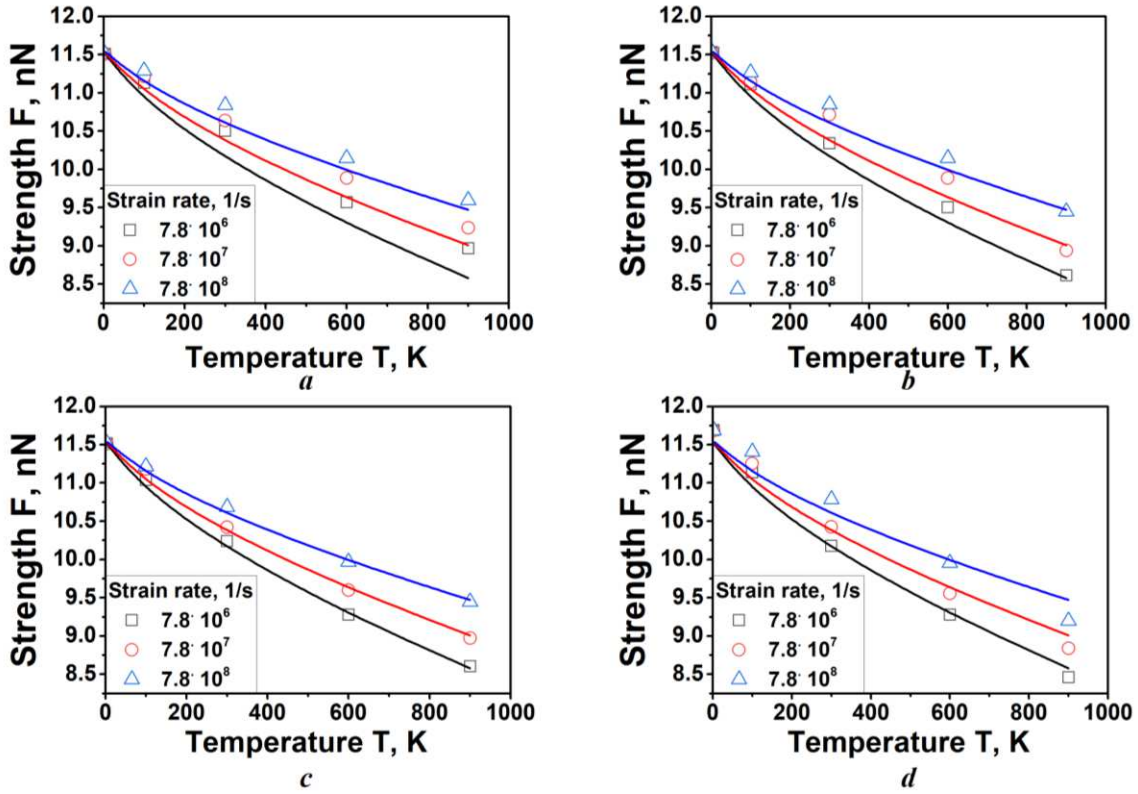


Fig. 6. Effect of temperature on the strength of the contact bond in the CGN for carbyne chains containing different numbers of atoms: (a) 6 atoms, (b) 10 atoms, (c) 14 atoms, and (d) 18 atoms. Symbols denote MD simulation data, and the solid line represents the theoretical curve.

Effects of Strain Rate:

On a logarithmic scale, the relationship between strength and strain rate at a fixed temperature is linear (Fig. 7), meaning that the underlying dependence is exponential.

According to the developed model, the effect of strain rate on strength is a consequence of a thermally activated mechanism of bond rupture at the contact points. In particular, this is also reflected in the fact that as temperature decreases, the influence of strain rate on strength diminishes. This occurs because the strain rate controls the time available for waiting for a critical fluctuation necessary to break an atomic bond. As temperature decreases, the probability of such a critical fluctuation occurring decreases, and consequently, the waiting time for the fluctuation increases. As a result, the force required to break the bond grows. To some extent, this can be interpreted as an increase in the athermal component of strength. The limiting strain rate $\dot{\varepsilon}_{ul}$ at which temperature ceases to affect strength, can be obtained from the diagram shown in Fig. 8. Physically, $\dot{\varepsilon}_{ul}$ characterizes the strain rate at which the time to failure is shorter than the waiting time for a critical fluctuation.

According to the data in Figs. 1 and 4, the limiting strain to reach F_{un} is $\varepsilon_{un} = 0.28$. Then, at the limiting strain rate $\dot{\varepsilon}_{ul} \approx 2.9 \cdot 10^{13} s^{-1}$ the limiting waiting time for the rupture of a contact bond $\tau_{ul} = \frac{\varepsilon_{un}}{\dot{\varepsilon}_{ul}} \approx 0.01 ps$. This value characterizes the lower bound of the waiting time for a critical fluctuation.

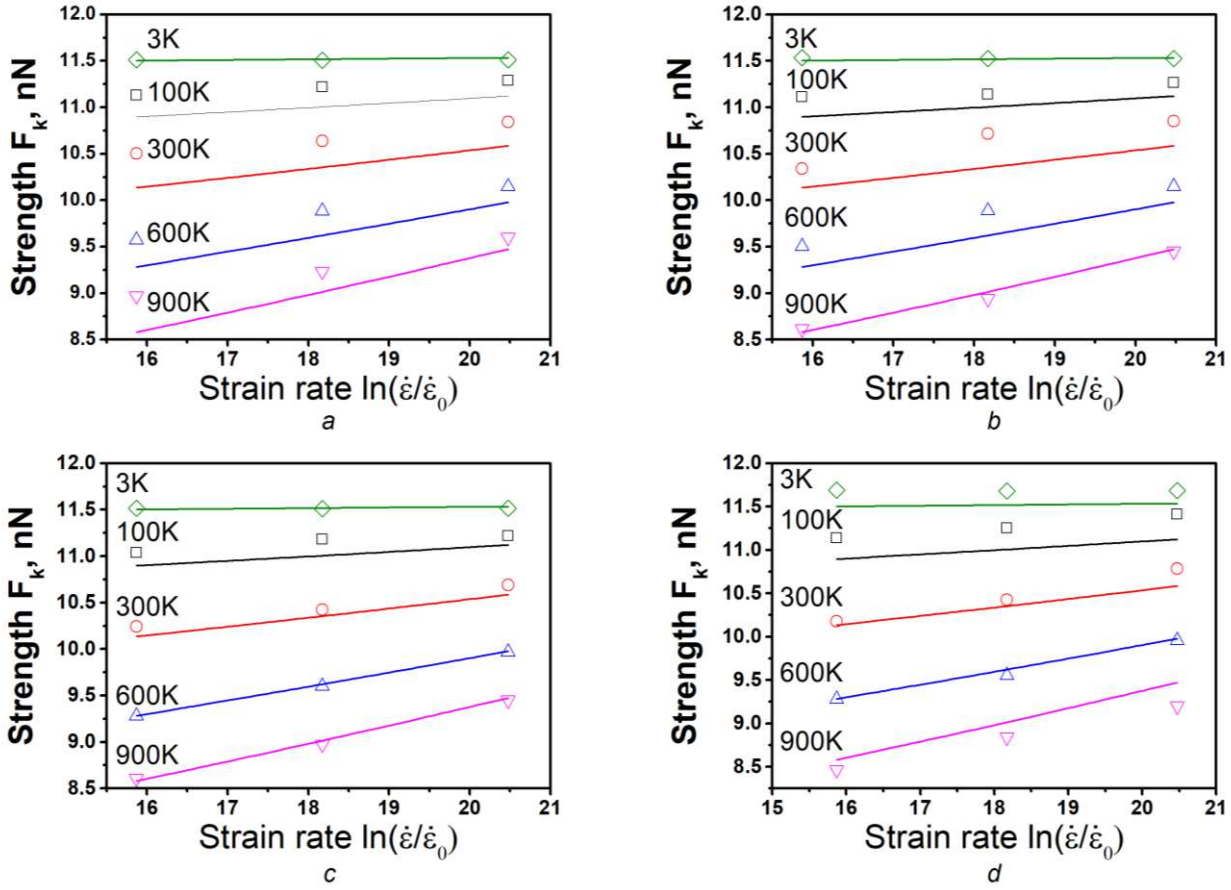


Fig. 7. Effect of strain rate on the strength of the contact bond in CGNs with carbyne chains containing different numbers of atoms in the temperature range 3–900 K: (a) 6 atoms, (b) 10 atoms, (c) 14 atoms, (d) 18 atoms; solid lines – theoretical predictions; symbols – MD simulation results. $\dot{\varepsilon}_0 = 1s^{-1}$is a reference strain rate.

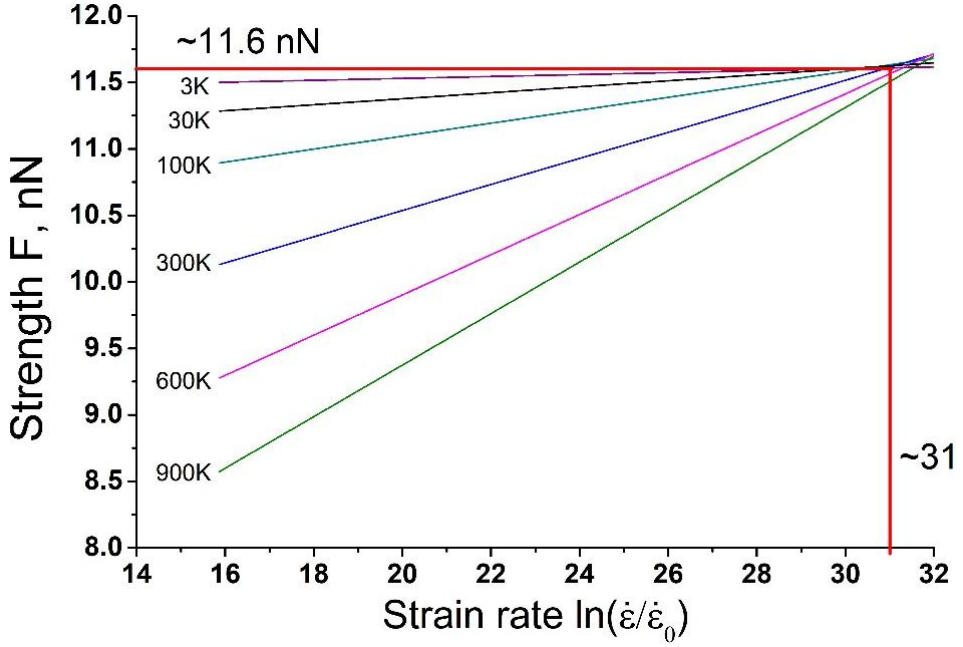


Fig. 8. Theoretical dependence of CGN strength on strain rate at different constant temperatures. $\dot{\varepsilon}_0 = 1s^{-1}$is a reference strain rate.

Effect of Chain Length:

According to the MD simulation results, increasing the chain length leads to a higher temperature sensitivity of strength; however, this effect is rather small: the difference between chains containing 6 and 18 atoms at 900 K is about 5%.

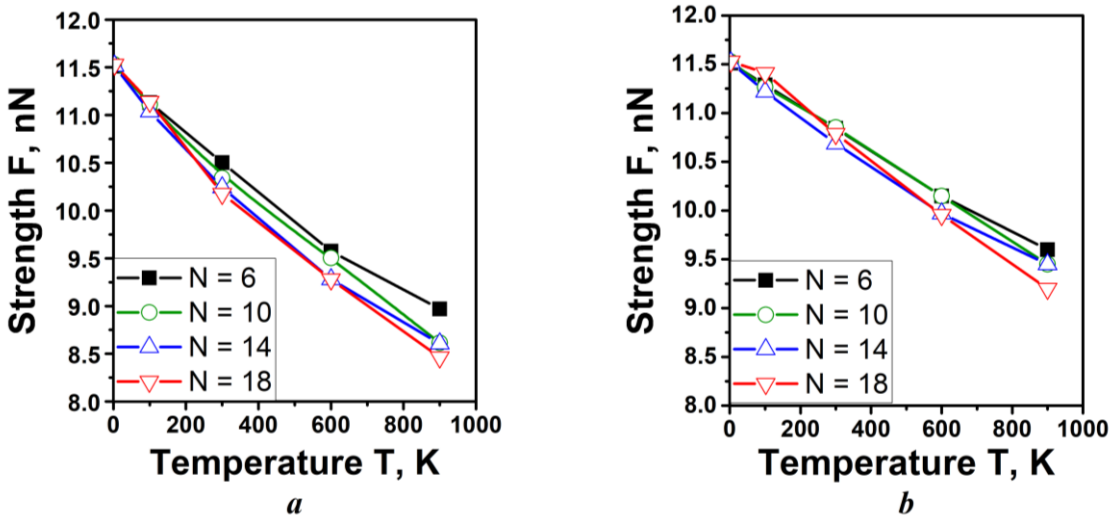


Fig. 9. Effect of the number of atoms, N, in the carbyne chain on strength at different chain strain rates: (a) $7.8 \cdot 10^6 s^{-1}$; (b) $7.8 \cdot 10^8 s^{-1}$

The obtained value is significantly smaller than the 16% reported by the authors in [30] for chains with n = 6 and n = 12. A likely reason for this discrepancy is the difference in the interatomic potentials used. As the authors themselves note in [30], their results deviate from DFT calculations, whereas in the present work the ACE potential was employed, providing the best agreement with DFT results.

The obtained results also differ from those reported in [40], where it was shown that strength decreases with increasing chain length inversely proportional to the number of atoms. At the same time, it should be taken into account that the object studied in our work is fundamentally different, as it is not an isolated carbyne chain. In the present case, the ultimate strength is determined by the strength of the contact bond. Under such conditions, the effect of chain length is minimal. The differences observed at high temperatures are likely associated with differences in the vibrational spectra of chains of different lengths, which in turn affect the fluctuation amplitude and the waiting time for their realization.

Conclusions:

1. The strength of carbyne–graphene nanoelements and similar nanoelements composed of combinations of one- and two-dimensional nanostructures is governed by the thermally activated rupture of the contact bond, which is responsible for its dependence on temperature and strain rate.

2. In semi-logarithmic coordinates, the strength of carbyne–graphene nanoelements increases linearly with the logarithm strain rate. The strain-rate sensitivity of strength depends on temperature and increases as temperature rises. When the strain rate increases by three orders of magnitude, the strength increases by 1.4% at 100 K, 3.1% at 300 K, and 6.5% at 900 K.
3. In the temperature range of 3–900 K, the strength of CGNs decreases with increasing temperature, with the total reduction not exceeding 20%. In terms of magnitude, this is close to the corresponding value reported for graphene (27%), but significantly

smaller than that observed for metallic nanowires (50%). This comparatively weak temperature effect is primarily due to the high stiffness of sp bonds.

4. It has been established that the effect of strain rate on strength has a thermally activated nature and is determined by the probability of the occurrence of a critical fluctuation required for atomic bond rupture. As temperature decreases, this effect becomes weaker, and at the limiting strain rate $\dot{\varepsilon}_{ul}$, temperature practically ceases to affect strength, since the time to failure becomes comparable to the atomic vibration period.
5. The influence of temperature and strain rate on the strength of carbyne-graphene nanoelements is governed by the thermally fluctuation nature of contact bond rupture. Temperature determines the magnitude of interatomic distance fluctuations, while the strain rate controls the time "allotted" for critical fluctuations to occur.
6. At temperatures not exceeding 300 K, variation of the carbyne chain length within the range of 8 – 23 Å (corresponding to 6 to 18 atoms) has virtually no effect on the strength of CGNs or on its sensitivity to temperature and strain rate. A slight effect of chain length, not exceeding 5%, observed at higher temperatures may be associated with changes in the amplitude–frequency characteristics of chain vibrations as the chain length varies.
7. The low sensitivity of CGN strength to temperature and strain rate supports the efficiency of their use as elements of straintronics.

Funding
This work was supported by the National Academy of Sciences of Ukraine [project number 0126U001813].

Ethics, Consent to Participate, and Consent to Publish declarations: not applicable.

References

1. Romdhane FB, Adjizian JJ, Charlier JC, Banhart F. Carbon. 2017. https://doi.org/10.1016/j.carbon.2017.06.039
2. Sarwat SG, Gehring P, Hernandez GR, Warner JH, Briggs GAD, Mol JA, Bhaskaran H. Nano Lett. 2017. https://doi.org/10.1021/acs.nanolett.7b00909
3. Cretu O, Botello-Mendez AR, Janowska I, Pham-Huu C, Charlier JC, Banhart F. Nano Lett. 2013. https://doi.org/10.1021/nl4018918
4. Shen L, Zeng M, Yang S, Zhang C, Wang X, Feng Y. J Am Chem Soc. 2010;132:11481–11486. https://doi.org/10.1021/ja909531c
5. La Torre A, Botello-Mendez A, Baaziz W, Charlier JC, Banhart F. Nat Commun. 2015;6:6636. https://doi.org/10.1038/ncomms7636
6. Zhang Z, Zhang J, Kwong G, Li J, Fan Z, Deng X, Tang G. Sci Rep. 2013;3:2575. https://doi.org/10.1038/srep02575
7. Gao E, Guo Y, Wang Z, Nielsen S, Baughman R. Matter. 2022;5(4). https://doi.org/10.1016/j.matt.2022.01.021
8. Liu M, Artyukhov VI, Lee H, Xu F, Yakobson BI. ACS Nano. 2013;7(11):10075–10082. https://doi.org/10.1021/nn404177r
9. He Y, Xu H, Ouyang G, Yang G. Results Phys. 2022. https://doi.org/10.1016/j.rinp.2022.105311
10. Chen T, Luo Y. Mon Not R Astron Soc. 2019;486(2):1875–1881. https://doi.org/10.1093/mnras/stz1014
11. Kano E, Takeguchi M, Fujita J, Hashimoto A. Carbon. 2014;80. https://doi.org/10.1016/j.carbon.2014.08.077
12. Jeevanandham S, Kochhar D, Agrawal O, Pahari S, Kar C, Goswami T, Sulania I, Mukherjee M. Nanoscale Adv. 2024. https://doi.org/10.1039/d4na00076e
13. Pereira VM, Neto AC. Phys Rev Lett. 2009;103:046801. https://doi.org/10.1103/PhysRevLett.103.046801
14. Zhan D, Yan J, Lai L, Ni Z, Liu L, Shen Z. Adv Mater. 2012;24:4055–4069. https://doi.org/10.1002/adma.201200011

15. Naumis GG, Roman-Taboada P. Phys Rev B. 2014;89:241404. https://doi.org/10.1103/PhysRevB.89.241404
16. Lin ZZ, Yu WF, Wang Y, Ning XJ. Europhys Lett. 2011;94:40002. https://doi.org/10.1209/0295-5075/94/40002
17. Ravagnan L, Piseri P, Bruzzi M, Miglio S, Bongiorno G, Baserga A, Casari CS, Li Bassi A, Lenardi C, Yamaguchi Y, Wakabayashi T, Bottani CE, Milani P. Phys Rev Lett. 2007;98:216103. https://doi.org/10.1103/PhysRevLett.98.216103
18. Zanolli Z, Onida G, Charlier JC. ACS Nano. 2010;4(9):5174–5180. https://doi.org/10.1021/nn100712q
19. Casari CS, Tommasini M, Tykwinski RR, Milani A. Nanoscale. 2016;8:4414–4435. https://doi.org/10.1039/C5NR06175J
20. Arrhenius S. Z Phys Chem. 1889;4:96–116. https://doi.org/10.1515/zpch-1889-0408
21. Arrhenius S. Z Phys Chem. 1889;4:226–248. https://doi.org/10.1515/zpch-1889-0416
22. Kramers HA. Physica. 1940;7:284–304. https://doi.org/10.1016/S0031-8914(40)90098-2
23. Smith IWM. Chem Soc Rev. 2008;37:812–826. https://doi.org/10.1039/B704257B
24. Zhurkov SN. Int J Fract Mech. 1965;1:311–323. https://doi.org/10.1007/BF03545562
25. Yang X, Huang Y, Cao B, To AC. Physica E. 2017;93:124–131. https://doi.org/10.1016/j.physe.2017.06.006
26. Zhu T, Li J, Samanta A, Leach A, Gall AK. Phys Rev Lett. 2008;100:025502. https://doi.org/10.1103/PhysRevLett.100.025502
27. Dumitrica T, Hua M, Yakobson BI. Proc Natl Acad Sci USA. 2006.
28. Kotrechko S, Stetsenko N, Kolyvoshko E. Solid State Phenom. 2016;258:286–289. https://doi.org/10.4028/www.scientific.net/ssp.258.286
29. Kotrechko S, Timoshevskii A, Kolyvoshko E, Matviychuk Y, Stetsenko N. Procedia Struct Integr. 2020;28:116–123. https://doi.org/10.1016/j.prostr.2020.10.015
30. Kotrechko S, Kolyvoshko E, Stetsenko N, et al. Appl Nanosci. 2023;13:4841–4855. https://doi.org/10.1007/s13204-022-02629-w

31. Drautz R. Phys Rev B. 2019;99:014104. https://doi.org/10.1103/PhysRevB.99.014104

32. Lysogorskiy Y, van der Oord C, Bochkarev A, Menon S, Rinaldi M, Hammerschmidt T, Mrovec M, Thompson A, Csanyi G, Ortner C, Drautz R. npj Comput Mater. 2021;7:97. https://doi.org/10.1038/s41524-021-00559-9

33. Thompson AP, Aktulga HM, Berger R, et al. Comput Phys Commun. 2022;271. https://doi.org/10.1016/j.cpc.2021.108171

34. Timoshevskii A, Kotrechko S, Matviychuk Y, Kolyvoshko E. In: Handbook of Graphene. 2019. https://doi.org/10.1002/9781119468455.ch58

35. Qamar M, Mrovec M, Lysogorskiy Y, Bochkarev A, Drautz R. arXiv:2210.09161

36. Hoover WG, Holian BL. Phys Lett A. 1996. https://doi.org/10.1016/0375-9601(95)00973-6

37. Zhou M. Proc R Soc A. 2003;459:2347–2392. https://doi.org/10.1098/rspa.2003.1127

38. Kotrechko S, Timoshevskii A, Kolyvoshko E, et al. Nanoscale Res Lett. 2017;12:327. https://doi.org/10.1186/s11671-017-2099-4

39. Zhao H, Aluru NR. J Appl Phys. 2010;108:064321. https://doi.org/10.1063/1.3488620

40. Wang Y, Ning XJ, Lin XZ, Li P, Zhuang J. Phys Rev B. 2007;76:165423. https://doi.org/10.1103/PhysRevB.76.165423